

Experimental band structure of Cu_3Au

Z. Q. Wang,* S. C. Wu,* J. Quinn, C. K. C. Lok, Y. S. Li, and F. Jona

College of Engineering and Applied Science, State University of New York, Stony Brook, New York 11794-2200

J. W. Davenport

Department of Physics, Brookhaven National Laboratory, Upton, New York 11973-5000

(Received 22 March 1988)

Angle-resolved photoemission experiments on $\text{Cu}_3\text{Au}\{001\}$ with synchrotron light in the range 12.5–46 eV are presented and evaluated to produce the band structure along $\Gamma-X$. The initial-band positions have been obtained by assuming free-electron-like final states. The experimental band structure is compared with a recently calculated band structure. Similarities and discrepancies are discussed.

I. INTRODUCTION

The determination of the dispersion of bulk bands in crystals by means of angle-resolved photoemission is a well-known and tested technique that has been described in several review articles.^{1,2} Of particular interest to the work described below are the studies on Cu by Knapp *et al.*³ and by Thiry *et al.*,⁴ and on Al by Levinson *et al.*⁵ Common to these studies is the fact that the determination of bulk energy-band dispersions from the observed interband transitions was done with the help of free-electron-like final bands shifted only by a constant inner potential, at least at relatively high photon energies ($h\nu > 35$ eV).

We report below experimental results and associated evaluations of these results that were aimed at the determination of bulk energy-band dispersions in ordered Cu_3Au , a classic ordering alloy that has been intensively studied by x-ray diffraction.⁶ Although no direct experimental measurement of the band structure of ordered Cu_3Au has been reported to date, a study of the optical absorption was carried out by Skriver and Lengkeek⁷ and compared with *ab initio* calculations. The optical measurements were done at 30 K with a direct ellipsometric technique between 0.5 and 5.3 eV. The electronic structure was calculated by means of the relativistic linear muffin-tin orbital method. The calculations revealed that ordered Cu_3Au has distinct Cu and Au *d* bands positioned in and hybridizing with an *s* band common to Cu and Au. Also, the order-disorder transition at 660 K has been studied with angle-resolved photoemission and Korringa-Kohn-Rostoker coherent-potential-approximation calculations by Jordan *et al.*⁸ Recently, ultraviolet⁹ and x-ray¹⁰ photoemission experiments have been performed on single crystals and for normal emission. On one hand Eberhardt and co-workers⁹ have argued that the spectra resemble those of isolated gold atoms in a copper matrix in that there are peaks in the range -4 to -7 eV which are separated by roughly the spin-orbit splitting in atomic gold. On the other hand, Wertheim¹⁰⁻¹² and co-workers have argued that the gold and copper bands are heavily hybridized, as would be ex-

pected for two noble metals, and that the spectra have, roughly, comparable gold and copper weights at all energies.

In order to address this issue we have undertaken to measure the bands using angle-resolved photoemission in the range 12.5–46 eV and to compare the results with a recent self-consistent band-structure calculation.¹³ The calculations show that the peaks between -4 and -7 eV have the bulk of their weight on the gold atoms. This conclusion is indicated by various population analyses and by the magnitude of the spin-orbit splitting, which is mostly determined by the (heavier) gold. The same analysis shows that the peaks above -4 eV have most of their weight on the copper atoms. In fact, the energy bands in this region resemble “folded-back” fcc copper *d* bands, and the spin-orbit splitting of these bands is small.

We describe in Sec. II the experimental procedure and in Sec. III the calculational procedure followed in order to extract the initial-state dispersion from the experimental curves. In Sec. IV we review the results of the band structure calculated by Davenport, Watson, and Weinert,¹³ and in Sec. V we discuss the comparison between experimental and theoretical band structure.

II. EXPERIMENTAL PROCEDURE

The sample (a single-crystal Cu_3Au platelet with a polished major surface in a $\{001\}$ plane) was wrapped in Ta foil adjacent to a $\text{Cu}\{001\}$ platelet and a polycrystalline Au foil. The Cu and Au samples were used as references. All three samples could be heated by sending electric current through the Ta foil. The assembly was mounted in a sample manipulator that allowed translations and rotations such that any one of the three samples could be exposed, in turn, to the photon beam, and the sample orientations could be varied with respect to the beam. The surfaces of all three samples were cleaned *in situ* [inside a vacuum chamber kept during the measurements at about $(5-9) \times 10^{-10}$ torr] by means of successive 1-h-long Ar-ion bombardments (5×10^{-5} torr of Ar, 500-eV Ar-ion energy, $5 \mu\text{A}/\text{cm}^2$ current) of the samples kept at 400–500 °C followed by 30-min anneals at 500 °C. The chemical composition of the surfaces was checked by

means of Auger-electron spectroscopy (AES) and the crystallinity of the Cu₃Au and the Cu samples was checked by low-energy electron diffraction (LEED). The cleaning process was continued until no carbon AES signal was detected on the surface to be studied.

The photoemission experiments were carried out at beam line U7 of the National Synchrotron Light Source (NSLS). A plane-grating monochromator (PGM) was used to disperse the synchrotron light and the experiments were carried out in the range of photon energies from 12.5 to 46 eV. The photon beam was incident onto the Cu₃Au surface at an angle of approximately 50° with respect to the surface normal, the electric vector of the light being almost parallel to a $\langle 110 \rangle$ direction of the Cu₃Au surface. The experiments were done in an angle-resolved mode with a hemispherical analyzer (Vacuum Generator) featuring a 2.4° acceptance angle and a total resolution of 0.3 eV as determined at the Fermi level of Au. Electron-distribution curves were measured for electrons emitted in the direction of the surface normal (normal emission). The geometry for normal emission, i.e.,

the position of the analyzer relative to the sample surface, was established by searching for extrema in the binding energy of selected pronounced peaks.

III. EVALUATION PROCEDURE AND RESULTS

Electron-distribution curves were measured from Cu₃Au{001} at normal emission for all photon energies in the range 12.5–46 eV as listed in Table I. Only some of these curves are depicted in Fig. 1. Table I summarizes the photon energies used and the associated binding energies of identifiable bands.

To analyze these results we draw first a “free-electron band structure” (more properly called an empty-lattice band structure) appropriate for Cu₃Au along the Γ - X direction of the Brillouin zone. We do not show this plot here; a similar one can be found, e.g., in Fig. 3 of Ref. 5. We then search in Fig. 1(b) for an extremum in binding energy of any band, and we find one at 20–22-eV photon energy for the band with 3.5-eV binding energy (see also Table I). The resulting kinetic energy of approximately

TABLE I. Experimental photoemission peak positions from Cu₃Au{001}. $h\nu$ is the photon energy in eV; E_b is the binding energy in eV. An asterisk denotes binding energies that are weak or cannot be resolved.

$h\nu$	E_b	$h\nu$	E_b	$h\nu$	E_b	$h\nu$	E_b
12.5	0.50	18.5	6.00	25.0	2.50*	35.0	6.90*
12.5	2.50	18.5	6.95	25.0	2.95	36.0	2.60*
13.0	0.60	19.0	2.80	25.0	3.55	36.0	3.30
13.0	2.55	19.0	3.50	25.0	5.40*	36.0	5.10
13.5	0.70	19.0	6.10*	25.0	6.10*	36.0	6.20
13.5	2.60	19.0	6.90	25.0	6.90*	36.0	6.85*
14.0	0.80*	20.0	2.80	26.0	3.00	38.0	2.00*
14.0	2.65	20.0	3.55	26.0	3.50	38.0	2.60*
14.5	2.65	20.0	3.95*	26.0	5.25*	38.0	3.30
14.5	3.20*	20.0	4.90*	26.0	6.05*	38.0	5.10*
15.0	2.70	20.0	6.00*	26.0	6.85*	38.0	6.30
15.5	2.40*	20.0	6.90	28.0	3.00*	38.0	6.90*
15.5	2.70	21.0	2.80	28.0	3.50	40.0	2.10*
15.5	3.00*	21.0	3.55	28.0	5.10*	40.0	3.20
15.5	6.00*	21.0	4.00*	28.0	6.75	40.0	5.10*
16.0	2.35*	21.0	5.00*	30.0	2.40*	40.0	6.25
16.0	2.75	21.0	5.80*	30.0	3.10*	40.0	6.75*
16.0	3.10*	21.0	6.85	30.0	3.50	42.0	2.50*
16.0	3.45*	22.0	2.80	30.0	5.00*	42.0	3.20
16.0	5.90	22.0	3.55	30.0	6.10*	42.0	5.10*
16.0	6.95*	22.0	3.90*	30.0	6.80	42.0	6.30
17.0	2.30*	22.0	5.15*	32.0	2.30*	42.0	6.70*
17.0	2.80	22.0	6.00*	32.0	3.40	44.0	2.50*
17.0	3.20	22.0	6.75	32.0	5.00	44.0	3.10
17.0	5.90	23.0	2.85	32.0	6.10*	44.0	3.50
17.0	7.00*	23.0	3.40	32.0	6.80	44.0	5.10
18.0	2.80	23.0	3.70*	34.0	2.10*	44.0	6.20
18.0	3.20	23.0	5.25*	34.0	3.40	44.0	6.90*
18.0	6.00	23.0	5.90*	34.0	5.10	46.0	2.40*
18.0	6.90	23.0	6.75	34.0	6.10	46.0	3.10
18.5	2.40*	24.0	2.85	34.0	6.80*	46.0	3.50
18.5	2.75	24.0	3.50	35.0	3.35	46.0	5.00
18.5	3.30	24.0	5.30*	35.0	5.05	46.0	6.20
18.5	5.10*	24.0	6.85*	35.0	6.20	46.0	6.90*

18 eV, when reported on the free-electron band-structure plot, indicates that this extremum must correspond to the X point at momentum $k_f = 3(\pi/a) = 2.51 \text{ \AA}^{-1}$. We can thus estimate the inner potential with the formula $k_f = 0.512(h\nu - E_i + |V_0|)^{1/2}$ (Ref. 1) where $h\nu$ is the photon energy, E_i is the binding energy of the initial state, and V_0 the inner potential (all in eV), and k_f is in units of \AA^{-1} . We thus obtain $V_0 = 6 \text{ eV}$. This estimate is not very accurate, to be sure, but is not too different from an estimate of V_0 obtained from LEED.¹⁴ We will take, then, $V_0 = 6 \pm 1 \text{ eV}$, and use this value for the band-structure determination described below.

To calculate the momentum k of the initial state we have assumed that the final state is free-electron-like.

Thus, for each binding energy value listed in Table I we have calculated a k value with the free-electron formula

$$k = \left[\frac{2m}{\hbar^2} (h\nu - E_i + |V_0|) \right]^{1/2}.$$

Since all k values thus obtained fell outside the first Brillouin zone, we then calculated the equivalent value of the momentum in the first Brillouin zone by subtracting appropriate reciprocal-lattice vectors of the type $(0, 0, 2\pi n/a)$, and finally reduced the results to values varying between 0 (the Γ point) and 0.5 (the X point) in units of $2\pi/a$. The results are shown in Fig. 2 as solid or open circles. The solid circles originate from strong and

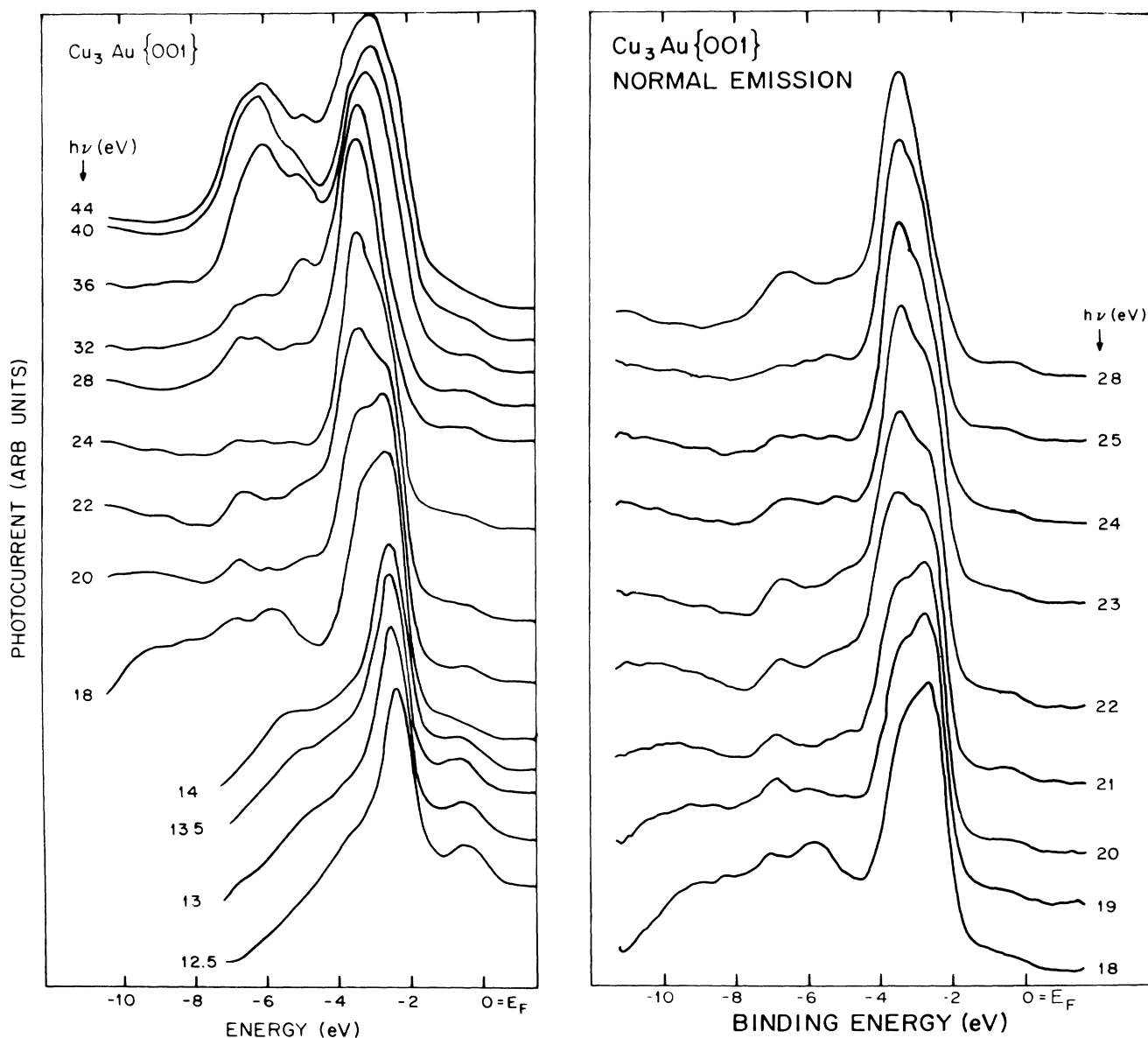


FIG. 1. Angle-resolved electron-distribution curves from Cu_3Au at normal emission. Left, photon energy $h\nu$ from 12.5 to 44 eV; right, photon energy $h\nu$ from 18.0 to 28 eV, sequence for the determination of the inner potential.

the nuclei. However, in contrast to other linear methods the calculations involve a Bloch sum of Slater-type orbitals to represent the wave function between the spheres. The calculation was iterated to self-consistency by means of the local-density-functional approximation for exchange and correlation. Only the muffin-tin part of the potential was used, and spin-orbit terms were neglected. [Recently, a similar scalar-relativistic calculation has been carried out¹² which used the full potential (no muffin-tin approximation). The results are similar to those published elsewhere¹³ and reported here.] Following the last iteration the spin-orbit interaction was included and the bands recalculated but not iterated to self-consistency. As described in detail elsewhere,¹⁵ The LASTO technique is comparable in accuracy to other *ab initio* band-structure methods though not as accurate as the linear-augmented-plane-wave (LAPW) method. The method has given good results for the heats of formation of other gold compounds as well.¹⁷

The resulting band structure is depicted in Fig. 2 without and with spin-orbit interactions, superimposed on the experimental results. The bands have been labeled according to the standard double-group notation.¹⁸

If the spin-orbit interaction could be neglected, then only states which are even or odd under the vertical mirror planes could be observed in normal emission.¹⁹ In the standard notation these are states with Δ_1 or Δ_5 symmetry. To aid thinking it is useful to introduce an explicit coordinate system and indicate which orbitals have Δ_1 or Δ_5 symmetry. Choosing the z axis perpendicular to the surface we find s , p_z , and d_{z^2} orbitals belonging to Δ_1 , and p_x , p_y , d_{xz} , and d_{yz} belonging to Δ_5 . The states with Δ_1 symmetry would be observed when the electric field of the incident light is normal to the surface and the states with Δ_5 symmetry would be observed when the electric field lies in the plane of the surface (s polarization). The other orbitals do not contribute to the normal emission. For the d bands these are $x^2 - y^2$ (Δ_2) and xy (Δ_2'). Addition of the spin-orbit interaction mixes the Δ_2 and Δ_2' into the Δ_5 states, and the resulting symmetry label is conventionally written Δ_7 . The Δ_1 states remain mixtures of s , p_z , and d_{z^2} only and are labeled Δ_6 . These are the only two irreducible representations and both would be observable in normal emission.

V. DISCUSSION

Experimentally, the energy bands of Cu_3Au appear to fall into two groups—those bands which lie below -5 eV and those which lie above -3.5 eV. According to the calculation¹³ the deeper bands are predominantly of gold character and the more shallow bands are predominantly copper. It is important to remember, however, that there is hybridization between the two groups so that there is some gold character at all energies. A Mulliken population analysis shows the bands between -5 and -7 eV are 65–85% gold.

It is not possible, however, to make a detailed compar-

ison between the calculated and experimental band structures. There appear to be many more bands in the calculation than have been observed experimentally. One possible explanation for this fact is the lack of experimental resolution. It shows that studies of metallic compounds with many atoms per unit cell require extremely high resolution to do the kind of band mapping which has become standard for elemental metals. Another possible explanation is the effect of the band folding. The bands in the region above -4 eV resemble those of fcc copper folded back into the simple-cubic Brillouin zone. Recall that the zone boundary for a fcc crystal is at $2\pi/a$ while for the simple-cubic structure it is at π/a . However, the intensity of the photoemission from these folded-back bands is expected to be low. In fact, if the gold were replaced by copper the intensity of the folded-back bands would be zero, and the gold potential is not expected to be very different from that of copper. Also, the selection rules for photoemission¹⁹ indicate that in the absence of spin-orbit coupling only Δ_1 and Δ_5 states contribute to the photocurrent normal to the surface. Spin-orbit coupling mixes the states so that all of them contribute. This is why they are all shown in Fig. 2. However, for small spin-orbit coupling (as is appropriate for copper) the states which are predominantly of Δ_2 and Δ_2' symmetry should be weak.

The most glaring discrepancy between theory and experiment in Fig. 2 is for the peak with binding energy of about -0.5 eV. There, no states approach the experimental points in the calculation. Indeed, in a fairly general way we can argue that the d bands of Cu_3Au should lie well below the Fermi level and the only states at -0.5 eV should be those in the broad s - p band which crosses the Fermi level about $\frac{1}{3}$ of the way to the zone boundary. This argument is consistent with Fermi-surface studies.²⁰ One possibility is that the observed peak is a surface state, but this possibility is very unlikely as this peak shows some dispersion (about 0.2 eV) and a peak at the same energy has been observed in pure copper.³ A more likely possibility is that the assumption of a free-electron final state, used to determine k , is not valid. The state is only observed for small photon energies, which means low final-state energies where the free-electron approximation could break down.

In summary, our angle-resolved photoemission measurements on Cu_3Au are consistent with first-principles electronic-structure calculations. The peaks in the energy-distribution curves fall into two groups which the calculation identifies as predominantly goldlike and predominantly copperlike. Detailed comparison of the theoretical and experimental bands is not possible because of the large number of bands predicted for a material with four atoms per unit cell. It would be useful experimentally to vary the angle of incidence of the light in order to identify the symmetry of the observed peaks. It would be useful theoretically to estimate the matrix elements so that a rough idea of the intensities of the various peaks could be obtained. At the lower photon energies the assumption of free-electron final states is probably not valid. Therefore calculations of the empty states above the Fermi level would also be useful.

ACKNOWLEDGMENTS

The experimental work was sponsored in part by the U.S. Department of Energy with Grant No. DE-FG02-86ER45239. The theoretical work was supported by the

Direction of Materials Sciences, U.S. Department of Energy, under Contract No. DE-AC02-76CH00016, and by a grant of computer time at the National Magnetic Fusion Energy Computing Center, Livermore, California.

*On leave from the Department of Physics, Peking University, Beijing, 100 871, The People's Republic of China.

¹D. E. Eastman and F. J. Himpsel, in *Physics of Transition Metals*, edited by P. Rhodes (IOP, London, 1981), p. 115.

²E. W. Plummer and W. Eberhardt, *Advances in Chemical Physics* (Wiley, New York, 1982), Vol. 49, p. 533.

³J. A. Knapp, F. J. Himpsel, and D. E. Eastman, *Phys. Rev. B* **19**, 4952 (1979).

⁴P. Thiry, D. Chandesris, J. Lecante, C. Guillot, R. Pinchaux, and Y. Petroff, *Phys. Rev. Lett.* **43**, 82 (1979).

⁵H. J. Levinson, F. Greuter, and E. W. Plummer, *Phys. Rev. B* **27**, 727 (1983).

⁶See, e.g., B. E. Warren, *X-Ray Diffraction* (Addison-Wesley, Reading, 1969), Chap. 12.

⁷H. L. Skriver and H. P. Lengkeek, *Phys. Rev. B* **19**, 900 (1979).

⁸R. G. Jordan, G. S. Sohal, B. L. Gyorffy, D. J. Durham, W. M. Temmerman, and P. Weinberger, *J. Phys. F* **15**, L135 (1985).

⁹W. Eberhardt, S. C. Wu, R. Garrett, D. Sondericker, and F. Jona, *Phys. Rev. B* **31**, 8285 (1985).

¹⁰S. B. DiCenzo, P. H. Citrin, E. H. Hartford, Jr., and G. K.

Wertheim, *Phys. Rev. B* **34**, 1343 (1986).

¹¹G. K. Wertheim, *Phys. Rev. B* **36**, 4432 (1987).

¹²G. K. Wertheim, L. F. Mattheiss, and D. W. E. Buchanan (unpublished).

¹³J. W. Davenport, R. E. Watson, and M. Weinert, *Phys. Rev. B* **37**, 9985 (1988).

¹⁴D. Sondericker, F. Jona, and P. M. Marcus (unpublished). Note that in LEED work the inner potential is usually referred to the vacuum level, whereas in photoemission work it is usually referred to the Fermi level. The difference between the two is the work function (4–5 eV).

¹⁵J. W. Davenport, M. Weinert, and R. E. Watson, *Phys. Rev. B* **32**, 4876 (1985).

¹⁶O. K. Andersen, *Phys. Rev. B* **12**, 3060 (1975).

¹⁷R. E. Watson, J. W. Davenport, and M. Weinert, *Phys. Rev. B* **35**, 508 (1987).

¹⁸R. J. Elliot, *Phys. Rev.* **96**, 280 (1954).

¹⁹J. Hermanson, *Solid State Commun.* **22**, 9 (1977).

²⁰P. P. Deimel and R. J. Higgins, *Phys. Rev. B* **25**, 7117 (1982).